1-1-2017

Use of Redox Probes for Characterization of Layer-by-Layer Gold Nanoparticle-Modified Screen-Printed Carbon Electrodes

Gregory W. Bishop
East Tennessee State University, bishopgw@etsu.edu

Ben K. Ahiadu
East Tennessee State University

Jordan L. Smith
East Tennessee State University

Jeremy D. Patterson
East Tennessee State University

Citation Information

Bishop, Gregory W.; Ahiadu, Ben K.; Smith, Jordan L.; and Patterson, Jeremy D.. 2017. Use of Redox Probes for Characterization of Layer-by-Layer Gold Nanoparticle-Modified Screen-Printed Carbon Electrodes. *Journal of the Electrochemical Society*. Vol.164(2). B23-B28. https://doi.org/10.1149/2.0431702jes ISSN: 0013-4651

Use of Redox Probes for Characterization of Layer-by-Layer Gold Nanoparticle-Modified Screen-Printed Carbon Electrodes

Journal of The Electrochemical Society

OPEN ACCESS

Use of Redox Probes for Characterization of Layer-by-Layer Gold Nanoparticle-Modified Screen-Printed Carbon Electrodes

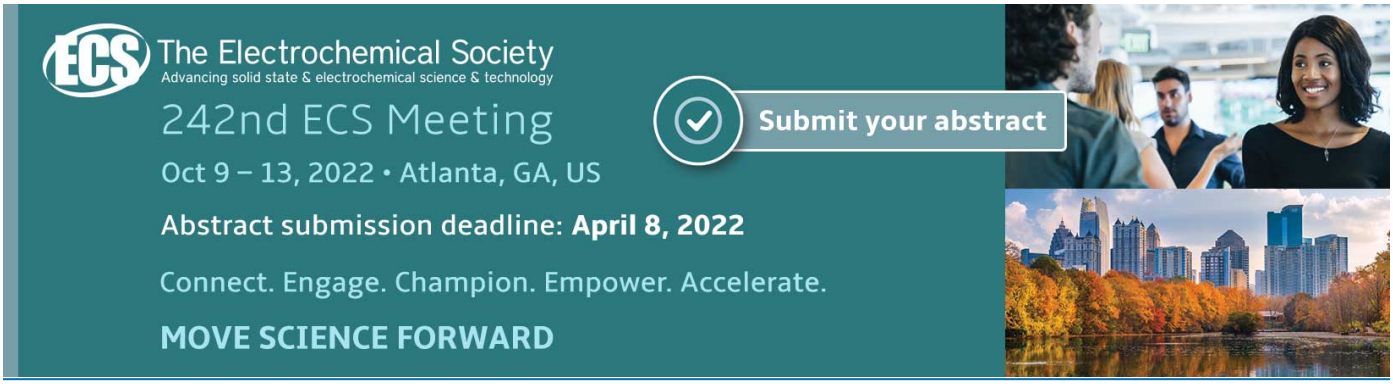

Use of Redox Probes for Characterization of Layer-by-Layer Gold Nanoparticle-Modified Screen-Printed Carbon Electrodes

Gregory W. Bishop,[*,z] Ben K. Ahiadu, Jordan L. Smith, and Jeremy D. Patterson

Department of Chemistry, East Tennessee State University, Johnson City, Tennessee 37614, USA

The electrochemical characteristics of bare and surface-modified screen-printed carbon electrodes (SPCEs) were compared using voltammetric responses of common redox probes to determine the potential role of nanomaterials in previously documented signal enhancement. SPCEs modified with gold nanoparticles (AuNPs) by layer-by-layer (LbL) electrostatic adsorption were previously reported to exhibit an increase in voltammetric signal for $Fe(CN)_6^{3-/4-}$ that corresponds to an improvement of 102% in electroactive surface area over bare SPCEs. AuNP-modified SPCEs prepared by the same LbL strategy using the polycation poly(diallyldimethylammonium chloride) (PDDA) here were found to provide no beneficial increase in electroactive surface area over bare SPCEs. Though similar improvement in voltammetric signal of $Fe(CN)_6^{3-/4-}$ was found for AuNP/PDDA-modified compared to bare SPCEs in these studies, results with other redox couples ferrocene methanol ($FcMeOH/FcMeOH^+$) and $Ru(NH_3)_6^{3+/2+}$ indicated no difference between the electroactive surface areas of modified and bare SPCEs. Furthermore, gold present on AuNP/PDDA-modified SPCEs accounted for only 62 (±12)% of the electroactive surface area. The previously reported improvement in electroactive surface area that was attributed to the inclusion of AuNPs on the SPCE surface appears to have resulted from a misinterpretation of the non-ideal behavior of $Fe(CN)_6^{3-}$ as a redox probe for bare SPCEs.

Manuscript received July 27, 2016. Published December 13, 2016.

Nanostructured electrodes have garnered a great amount of interest in the field of electrochemistry due to their interesting and sometimes superior properties compared to bulk analogs.[1] Nanomaterials have been widely used for the preparation of energy storage and conversion devices[2–5] as well as sensors, biosensors, and bioelectronics.[1,5–8] Such applications have largely been driven by the advantageous properties of nanomaterials, such as their large surface areas, electrocatalytic capabilities, and/or abilities to facilitate electron transport between bulk materials and electrochemically active biological materials.

One simple and widely used technique for preparing nanostructured electrodes, called the layer-by-layer (LbL) method,[9] involves adsorption of successive layers or films of different materials onto an underlying conductive bulk surface.[5,6] Adjacent layers usually associate through electrostatic interactions between materials of opposite charge. Film stability can also be affected by other intermolecular forces such as hydrogen bonding, hydrophobic interactions, and Van der Waal's forces.[6] LbL-constructed nanostructured electrodes have found use in the preparation of supercapacitors[4,5] and proton-exchange membrane fuel cells (PEMFCs)[4] as well as chemical sensors and biosensors.[1,6–8]

Sensors and biosensors prepared by LbL methods often employ ionic polymers like poly(diallyldimethylammonium chloride) (PDDA) and/or polystyrene sulfonate (PSS) to facilitate adsorption of metal, semiconductor, or carbon-based nanoparticles (e.g., nanospheres, nanorods, nanotubes or graphene sheets) typically onto a bulk carbon or gold electrode. In addition to conventional disk-shaped glassy carbon, pyrolytic carbon, and gold electrodes, screen-printed electrodes have also found wide use as platforms for LbL-based sensors and biosensors. Screen printing enables low-cost, customizable sensor design and provides opportunities to tailor electrode properties through ink formulation and pattern geometry.[10–12] Inks for preparing screen-printed electrodes typically consist of conductive particles distributed with one or more polymeric binders (e.g., poly(vinyl chloride), poly(vinyl acetate), etc.) in a solvent (e.g., cyclohexanone, mesitylene, etc.).[10–15] Manual, semi-automatic, or automatic screen-printing may be employed using inks prepared from raw materials or purchased from commercial sources. Pre- and custom-designed screen-printed electrodes are also available from several manufacturers.

Application of LbL methods to screen-printed carbon electrodes (SPCEs) provides a relatively simple, cost-effective, and versatile strategy for producing nanomaterial-modified electrodes. When employed as platforms for sensing and biosensing, such electrodes reportedly exhibit improved electrochemical properties (e.g., enhanced response and/or superior electron-transfer kinetics over bare SPCEs).[7,8,16–18] One benefit provided by nanoparticles that is typically asserted as important in rationalizing the augmented response of nanomaterial-modified SPCEs over bare SPCEs is the increase in electroactive surface area provided by the inclusion of nanomaterials on the electrode surface.[7,8,16–18] The electroactive surface area, A, is often determined (in cm^2) through voltammetric studies of common redox probes by employing the Randles-Ševčík equation (at 25°C):[13,17,19]

$$i_p = \left(2.69 \times 10^5\right) n^{3/2} A D^{1/2} C v^{1/2} \quad [1]$$

where i_p is the peak current in amperes, n is the number of electrons involved in the electrode reaction, D is the diffusion coefficient (in $cm^2\ s^{-1}$) of the electroactive species (redox probe), C is the bulk concentration of the electroactive species (in mol cm^{-3}), and v is the scan rate (in V s^{-1}).[20] Using this method with $Fe(CN)_6^{3-/4-}$ as the redox probe, a previous report established that the electroactive surface area of SPCEs can be increased by 102% by employing an LbL strategy to modify the electrode surface with glutathione-capped gold nanoparticles (AuNPs).[17]

Recent studies with highly ordered pyrolytic graphite (HOPG) and graphene-modified electrodes have indicated that characterization of carbon electrodes through use of the $Fe(CN)_6^{3-/4-}$ redox couple can result in misinterpretation of their electrochemical properties.[21–23] For example, the cyclic voltammetric (CV) response of HOPG electrodes using 1 mM $Fe(CN)_6^{4-}$ in 0.1 M KCl was found to depend on time.[21] Freshly cleaved HOPG surfaces exhibited voltammetric peak-to-peak separation (ΔE_p) values near 59 mV as expected for an electrochemically reversible process, while aged HOPG surfaces produced much larger ΔE_p values and lower peak currents for the $Fe(CN)_6^{4-/3-}$ redox couple that are suggestive of poorer electron transfer kinetics. In contrast, similar experiments with $Ru(NH_3)_6^{3+/2+}$ did not indicate any significant difference between the electrochemical behaviors of freshly cleaved and aged HOPG electrodes. CV studies of graphene-modified electrodes using $Fe(CN)_6^{3-}$, $Ru(NH_3)_6^{3+}$, and ferrocene methanol (FcMeOH) produced similar results, with $Fe(CN)_6^{3-}$ exhibiting sensitivity to supporting electrolyte solution and electrode surface conditions that were not observed with either $Ru(NH_3)_6^{3+}$ or FcMeOH.[22]

Overall these studies suggest that the $Fe(CN)_6^{3-/4-}$ redox couple may be a poor choice for the electrochemical characterization of some carbon-based electrodes due to its somewhat unique surface sensitivity

*Electrochemical Society Member.
[z]E-mail: bishopgw@etsu.edu

compared to other common outer-sphere redox probes. This sensitivity can result in complicated, non-ideal, and unpredictable behavior.[24] Variations in the response of the $Fe(CN)_6^{3-/4-}$ redox couple on HOPG and graphene-modified electrodes have been used to help explain the wide disparities in reported electrochemical behaviors of carbon nanotubes and graphene as well as the perceived dependence of electrochemical properties of carbon materials on edge and basal plane surfaces and defects.[21–23] Such observations suggest that care must be taken when employing $Fe(CN)_6^{3-}$ as a redox probe to characterize the electrochemical properties of carbon-based electrodes.[21]

While the electrochemical characteristics of SPCEs have been widely reported, many of these studies have relied on interpretation of SPCE response with the $Fe(CN)_6^{3-/4-}$ redox couple.[13,17,18,25,26] Furthermore, the improvement in electroactive surface area previously reported for LbL construction of AuNP-modified SPCEs was based on differences between the CV responses of $Fe(CN)_6^{3-/4-}$ on AuNP-modified and bare SPCEs.[17,19] Here, we investigate the electrochemical responses of $Fe(CN)_6^{3-/4-}$ and other redox probes ($Ru(NH_3)_6^{3+}$ and FcMeOH) using bare and LbL-modified SPCEs to determine the importance and role of AuNPs in improving electrochemical properties of modified SPCEs. The extent of AuNP coverage and effect of AuNPs on the electroactive surface area of modified SPCEs are also addressed. The results of these studies may have wider implications to other types of modified SPCEs that are used as sensing platforms and the characterization of their electrochemical properties.

Experimental

Materials.—Potassium ferricyanide and sodium borohydride were obtained from Fisher Scientific. Ferrocene methanol and 20 wt% poly(diallyldimethylammonium chloride) (PDDA) solution (average MW 200,000-350,000) in water were obtained from Sigma-Aldrich. Hexaammineruthenium (III) chloride was purchased from Strem Chemicals. Hydrogen tetrachloroaurate (III) hydrate and L-glutathione were obtained from Alfa Aesar. All solutions were prepared using 18.2 MΩ · cm ultrapure water prepared by passing deionized water through a Millipore Synergy UV purification system. Screen-printable carbon graphite (C2050106D7) and Ag/AgCl (C2051014P10) inks were supplied by Gwent Electronic Materials Ltd (Pontypool, UK).

Fabrication of screen-printed carbon electrodes (SPCEs).—Electrodes were prepared from graphite and Ag/AgCl inks by manual screen printing using a 200 mesh screen coated with diazo photo emulsion. Patterns that define electrodes, conductive paths, and contact pads were printed on acetate tracing paper using an inkjet printer and placed under an 8 in. × 10 in. piece of glass on top of the photo emulsion-coated screen. Patterns were transferred to the screen by exposure using a 150 W clear incandescent bulb at a height of 18″ above the screen for 7 min.

Using a squeegee, graphite ink was forced through the screen and transferred onto a cellulose acetate sheet (transparency film) to produce contact pads, conductive paths for electrode connection, and working and counter electrodes. The pattern that defined graphite ink designs featured three 2 mm × 5 mm (w × l) contact pads each connected to a 1 mm × 20 mm conductive path, a circular 2 mm diameter working electrode connected to the center conductive path, and a 2 mm-wide arc-shaped counter electrode (inner arc radius 2 mm) connected to one of the outer conductive paths (Figure 1). Ink was cured in an oven for 30 min at 60°C. Ag/AgCl ink was forced through a 2 mm-wide arc-shaped pattern (inner arc radius 1 mm) on the screen to form the reference electrodes on top of the third conductive path. After Ag/AgCl ink deposition, curing was again carried out for 30 min at 60°C. Kapton tape was placed over printed conductive paths for insulation and to help define working electrode area. Geometric areas of working electrodes were measured from digital photographic images using ImageJ.[27] The average geometric area of the working electrodes used in electrochemical studies was 2.52 (±0.29) × 10^{-2} cm^2 ($n = 10$).

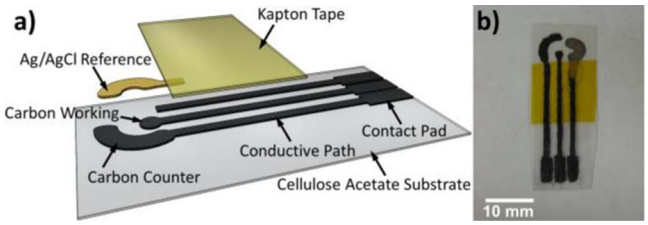

Figure 1. Exploded view of design (a) and photographic image (b) of screen-printed electrode.

Synthesis of glutathione-capped gold nanoparticles.—Glutathione (GSH)-capped gold nanoparticles (AuNPs) were prepared according to previous reports.[17,19] Briefly, 19.7 mg hydrogen tetrachloroaurate hydrate and 7.7 mg L-gluathione were dissolved in a mixture of methanol and acetic acid (86:14 by vol%). The solution was rapidly stirred using a magnetic stirrer, and 1.5 mL of a 0.53 mM sodium borohydride solution was added dropwise. Addition of the sodium borohydride solution was immediately accompanied by a change in color of the solution from bright yellow to brown. After 2 hours of continued stirring, the suspension was filtered through 50 kDa MW cutoff filter centrifuge tubes by centrifugation at 2150x*g* for 8 minutes. Particles were resuspended in 20 mM HEPES buffer, pH 8.0, and centrifugation was repeated four times followed by final resuspension in HEPES buffer. UV-Vis spectra of 10-fold diluted particle suspension exhibited a characteristic absorbance peak at 515 nm. Estimation of particle size from UV-Vis absorbance[28] indicated particle diameter of 4–5 nm, which is in agreement with similarly prepared particles in previous reports.[17,19]

Layer-by-layer deposition of AuNPs on SPCEs.—Screen-printed carbon electrodes (SPCEs) were pretreated by performing a linear voltammetric sweep from −1.2 to +1.5 V vs. Ag/AgCl at 100 mV s^{-1}.[25] After pretreatment, electrodes were rinsed with ultrapure water and dried. AuNPs were deposited on the SPCE via a previously reported layer-by-layer deposition technique.[17,19] A micropipette was used to deliver 2 μL of 2 mg mL^{-1} PDDA in 50 mM NaCl to the working electrode. After 20 minutes, the PDDA-modified electrode was rinsed with ultrapure water and dried. 2 μL of AuNP suspension was then added to the working electrode surface. After 20 minutes, the AuNP/PDDA-modified electrode was rinsed with ultrapure water to remove any excess AuNPs.

Electrochemical measurements.—All electrochemical measurements were performed using a CHI 400 operating in potentiostatic mode. Bare, PDDA-modified, and AuNP/PDDA-modified electrodes were placed in a 10 mL beaker filled with potassium ferricyanide, hexaammineruthenium (III) chloride, or ferrocene methanol (FcMeOH) in 0.1 M KCl, and cyclic voltammetry (CV) was performed at 10–200 mV s^{-1}. Measured currents were converted to current densities by normalization with the geometric area for each electrode.

Results

Cyclic voltammetry of common redox probes using bare and modified SPCEs.—Among the three redox probes used in these studies, the largest differences between bare and modified SPCEs were exhibited through use of $Fe(CN)_6^{3-}$ (Figure 2). For the $Fe(CN)_6^{3-/4-}$ redox couple, bare SPCEs presented smaller peak current densities ($j_p = i_p / A_{geo}$) (Table I) and larger ΔE_p (Table II) compared to PDDA- and AuNP/PDDA-modified SPCEs. While all ΔE_p values are significantly larger than 59 mV that is indicative of an electrochemically reversible process, 217 (± 49) mV for $Fe(CN)_6^{3-/4-}$ determined in these studies using bare SPCEs is comparable to the value found with analogous measurements (234 mV) using SPCEs that exhibited edge plane-like properties.[29]

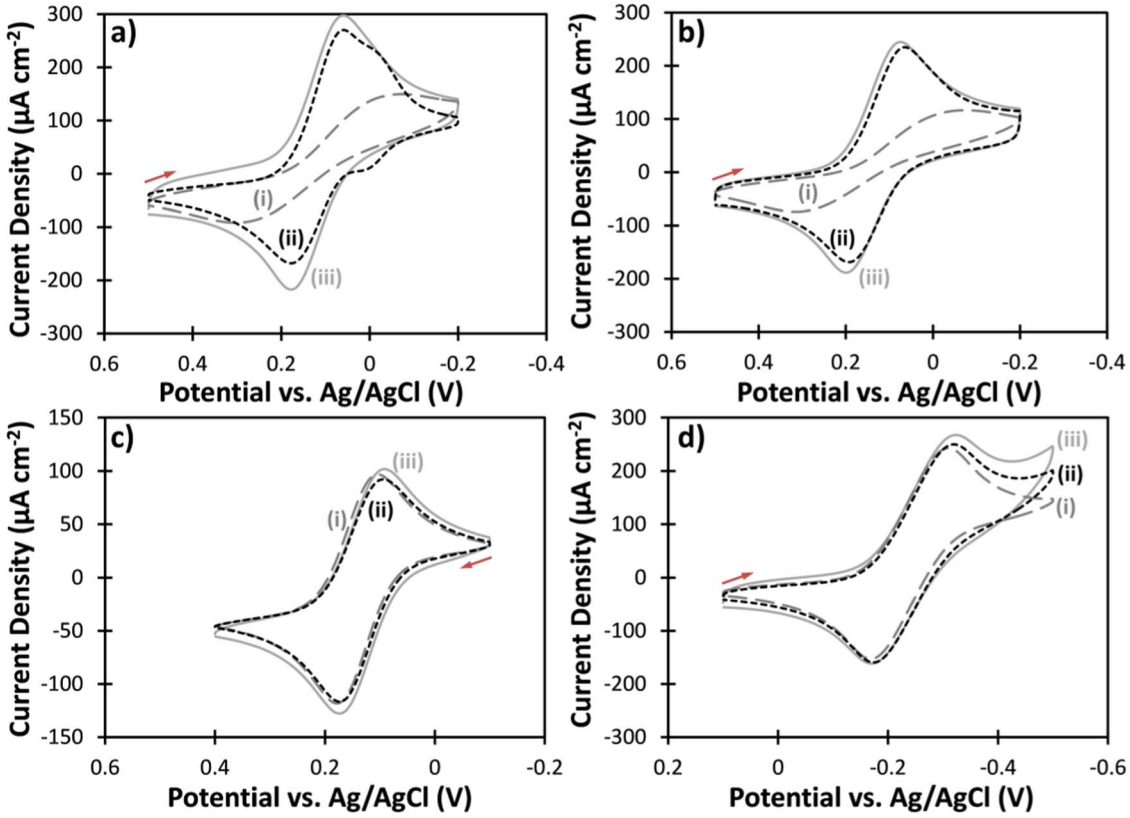

Figure 2. Representative CVs of 1 mM $K_3[Fe(CN)_6]$ (a, b), 0.5 mM FcMeOH (c), and 1 mM $[Ru(NH_3)_6]Cl_3$ (d) using bare (i), PDDA- (ii), and AuNP/PDDA-modified (iii) SPCEs in 0.1 M KCl at 100 mV s^{-1}. For CVs of 1 mM $K_3[Fe(CN)_6]$, typical response of PDDA-modified SPCEs (a) exhibited post-reduction and pre-oxidation waves, while atypical response produced no additional CV features (b). Arrows indicate direction of scans.

Table I. Peak current density (j_p) for forward voltammetric scans of various redox probes in 0.1 M KCl with bare and modified SPCEs using voltammetric scan rate of 100 mV s^{-1}.

	j_p (μA cm^{-2}) for Various Redox Probes		
SPCE Modification	1 mM $Fe(CN)_6^{3-}$	0.5 mM FcMeOH	1 mM $Ru(NH_3)_6^{3+}$
None (Bare)	138 (±18)	−126 (±6)	214 (±29)
PDDA	233 (±22)	−129 (±8)	215 (±32)
AuNP/PDDA	213 (±26)	−122 (±13)	223 (±23)

There were no significant differences between j_p and ΔE_p for the $Fe(CN)_6^{3-/4-}$ redox couple between PDDA- and AuNP/PDDA-modified SPCEs at the 95% confidence level. However, PDDA-modified SPCEs typically displayed post-reduction and pre-oxidation waves or peaks (Figure 2a) that were not present in CVs using AuNP-modified electrodes. Post- and pre-peak waves for the $Fe(CN)_6^{3-/4-}$ redox couple were evident for 70% (7 out of 10) of the PDDA-modified electrodes used in these studies. Even without this behavior, PDDA-modified electrodes still produced $Fe(CN)_6^{3-/4-}$ peak currents that were similar to those obtained using AuNP/PDDA-modified SPCEs (Figure 2b). In contrast to the $Fe(CN)_6^{3-/4-}$ redox couple, the $Ru(NH_3)_6^{3+/2+}$ and FcMeOH/$FcMeOH^+$ redox couples exhibited no significant differences for j_p or ΔE_p between bare, PDDA-modified, and AuNP/PDDA-modified electrodes at the 95% confidence level. However, j_p varied by as much as 15%, and ΔE_p varied by as much as 27% among electrodes with like surface modifications. These differences in j_p and ΔE_p as well as those in CVs of PDDA-modified electrodes may result from variations in the distribution of edge plane, basal plane, and polymeric domains[30] in the SPCEs due to ink inhomogeneity or inconsistencies in the manual screen printing process.

Table II. Peak separation (ΔE_p) for various redox couples in 0.1 M KCl with bare and modified SPCEs using voltammetric scan rate of 100 mV s^{-1}.

	ΔE_p (mV) for Various Redox Couples		
SPCE Modification	1 mM $Fe(CN)_6^{3-/4-}$	0.5 mM FcMeOH/$FcMeOH^+$	1 mM $Ru(NH_3)_6^{3+/2+}$
None (Bare)	217 (±49)	90 (±17)	109 (±29)
PDDA	133 (±30)	94 (±17)	113 (±25)
AuNP/PDDA	136 (±34)	102 (±18)	117 (±32)

Electroactive surface areas of bare and modified SPCEs.— Since ΔE_p values indicated electron transfer with all redox probes to be quasireversible, electroactive surface areas of bare and modified SPCEs were determined from a modified version of the Randles-Ševčík equation (Eq. 1):[20,26]

$$i_p = (2.69 \times 10^5)\, n^{3/2} A D^{1/2} C v^{1/2} K(\Lambda, \alpha) \quad [2]$$

where $K(\Lambda, \alpha)$ is a function that depends on the rate parameter Λ and the electron transfer coefficient α, which is taken to be 0.5 for the redox probes used in these studies.[13,31] The rate parameter Λ is related to the parameter ψ that is used to estimate the electron transfer rate constant k_0 (in cm s^{-1}) from CV measurements via the Nicholson method:[20,32]

$$\Lambda = \pi^{1/2}\, \psi = k_0 \left(D_O^{1-\alpha} D_R^{\alpha} n f v\right)^{-1/2} \quad [3]$$

where D_O and D_R are the diffusion coefficients of the oxidized and reduced forms of the redox probe, respectively, and f corresponds to

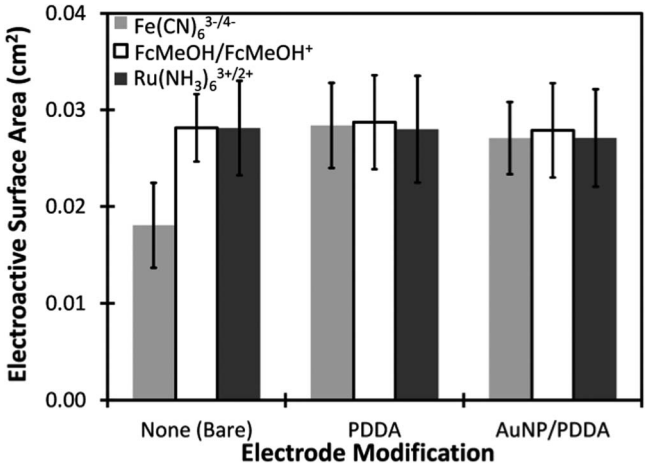

Figure 3. Average electroactive surface areas estimated for bare, PDDA-, and AuNP/PDDA-modified SPCEs by Eq. 2 using $Fe(CN_6)^{3-/4-}$ (light gray), $FcMeOH/FcMeOH^+$ (white), and $Ru(NH_3)_6^{3+/2+}$ (dark gray) as redox probes. Error bars represent one standard deviation ($n = 10$).

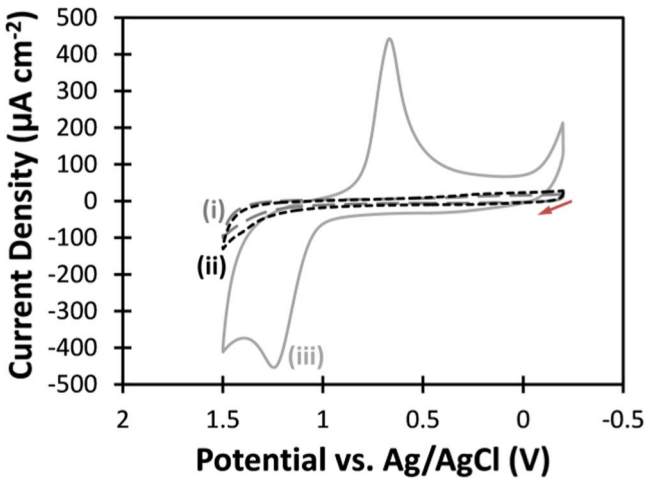

Figure 4. Representative CVs of bare (i), PDDA- (ii), and AuNP/PDDA-modified (iii) SPCEs in 0.5 M H_2SO_4 at 100 mV s^{-1}. Arrow indicates direction of scans.

$F(RT)^{-1}$, with F, R, and T representing Faraday's constant, the gas constant, and absolute temperature, respectively.

ψ was determined from ΔE_p with CVs obtained using scan rates v ranging from 10–200 mV s^{-1} as described by Nicholson.[32] Eq. 3 was employed to calculate Λ from ψ, and $K(\Lambda, \alpha)$ in Eq. 2 was determined from the work of Matsuda and Ayabe.[20,26,33] Electroactive surface areas for bare and modified SPCEs were then calculated using Eq. 2 based on literature values of 7.60×10^{-6}, 7.80×10^{-6}, and 8.43×10^{-6} cm^2 s^{-1} for the diffusion coefficients of $Fe(CN)_6^{3-}$,[13] FcMeOH,[34] and $Ru(NH_3)_6^{3+}$,[35] respectively (Figure 3).

The electroactive surface area calculated for bare SPCEs using $Fe(CN)_6^{3-}$ was 1.81 (±0.44) $\times 10^{-2}$ cm^2 (Figure 3), which is smaller than A_{geo} (2.52 (±0.29) $\times 10^{-2}$ cm^2). If the electroactive surface area determined by $Fe(CN)_6^{3-}$ is accepted, the deposition of PDDA on the electrode surface resulted in an increase in electroactive surface area of 61(±12)%. Similarly, AuNP/PDDA-modified SPCEs represent an increase in electroactive surface area of 54(±15)% over bare SPCEs. This increase in surface area is smaller than the 102% increase in surface area that was reported for similar AuNP/PDDA-modification of commercially available SPCEs,[17] and similar to the 44.8% increase in surface area afforded by analogous AuNP/PDDA-modification of glassy carbon electrodes.[19] However, it should be noted that the previous studies seem to have employed the reversible form of the Randles-Ševčík equation (Eq. 1) in the determination of the electroactive surface area, though ΔE_p appeared to indicate that the quasireversible form (Eq. 2) would be more appropriate. The use of Eq. 1 for the calculation of electroactive surface areas of SPCEs that exhibit quasireversible behavior is common.[13,31] A smaller surface area of 1.24 (±0.30) $\times 10^{-2}$ cm^2 is estimated for bare SPCEs when Eq. 1 is used with $Fe(CN)_6^{3-}$ data in these studies.

In contrast to the results obtained with $Fe(CN)_6^{3-}$, there were no differences between the calculated electroactive surface areas of bare, PDDA-, and AuNP/PDDA-modified SPCEs when FcMeOH or $Ru(NH_3)_6^{3+}$ was used as the redox probe (Fig. 3). Additionally, electroactive surface areas obtained for PDDA- and AuNP/PDDA-modified SPCEs using $Fe(CN)_6^{3-}$ were similar to those found using FcMeOH and $Ru(NH_3)_6^{3+}$. For all experiments besides bare SPCEs with $Fe(CN)_6^{3-}$, the average electroactive surface area of bare, PDDA-, and AuNP-modified SPCEs was determined to be 2.79 (±0.46) $\times 10^{-2}$ cm^2, which is slightly larger than A_{geo}.

Commercially available conductive graphitic screen-printing inks consist of a proprietary mixture of graphite particles, polymeric binder(s) (typically poly(vinyl chloride), poly(vinyl acetate), etc.), and solvent(s).[13] Commercially available SPCEs have been shown to consist of electroactive sites distributed within an electro-inactive matrix. The ratio of electroactive to geometric surface area ($R_A = A/A_{geo}$), also called the roughness factor, has been previously used to characterize SPCEs as a means to describe the extents of these electroactive and inactive domains.[13,31] Upon converting this ratio to a percentage for bare SPCEs, results with FcMeOH and $Ru(NH_3)_6^{3+}$ indicated R_A to be 113 (±5)% and 110 (±10)%, respectively. In contrast, an R_A value of 71(±10)% was obtained using the electroactive surface area determined from $Fe(CN)_6^{3-}$ experiments. Similar measurements for various commercially available SPCEs ranged from 39–79% using $Fe(CN)_6^{3-}$.[13]

Electron transfer kinetics.—Heterogeneous electron transfer rate constants k_0 were determined through the Nicholson method using the linear relationship between ψ and $v^{-1/2}$ (Eq. 3). The same literature values listed above for D in Eq. 2 were used for D_O for $Fe(CN)_6^{3-}$ and $Ru(NH_3)_6^{3+}$ and $D_O = D_R$ for FcMeOH in Eq. 3.[13,34–36] Literature values of 6.5×10^{-6} and 1.19×10^{-5} cm^2 s^{-1} were used for D_R of $Fe(CN)_6^{4-}$ and $Ru(NH_3)_6^{2+}$, respectively.[20,35] Surface modification did not appear to have an effect on k_0 for $FcMeOH/FcMeOH^+$ or $Ru(NH_3)_6^{3+/2+}$, as there were no differences between rate constants obtained with bare, PDDA-, and AuNP/PDDA-modified SPCEs. Rate constants for $FcMeOH/FcMeOH^+$ and $Ru(NH_3)_6^{3+/2+}$ were found to be 6.8 (±2.1) $\times 10^{-3}$ and 4.1 (±1.7) $\times 10^{-3}$ cm s^{-1}, respectively. Using $Fe(CN)_6^{3-/4-}$, there was no significant difference between k_0 values obtained with PDDA- and AuNP/PDDA-modified SPCEs. The average k_0 for $Fe(CN)_6^{3-/4-}$ using modified electrodes was found to be 2.9 (±1.2) $\times 10^{-3}$ cm s^{-1}, while a value of 1.20 (±0.25) $\times 10^{-3}$ cm s^{-1} was determined for k_0 for the same system with bare SPCEs. Electron transfer rate constants between 1.67×10^{-5} and 8.2×10^{-3} cm s^{-1} have been reported for $Fe(CN)_6^{3-/4-}$ using other SPCEs.[13,25,36,37]

Evaluation of AuNP surface coverage.—Voltammograms of AuNP/PDDA-modified SPCEs in 0.5 M H_2SO_4 exhibited characteristic peaks at +1.25 (±0.010) V and +0.66 (±0.025) V corresponding to the oxidation and subsequent reduction of AuNPs, respectively (Figure 4).[38,39] Surface areas attributed to AuNPs for AuNP/PDDA-modified SPCEs were estimated using the charge associated with the reduction peak at +0.66 (±0.025) V.[38–40] For a monolayer of gold, the integration of this reduction peak results in a charge of 400 µC cm^{-2}.[40] The surface area of AuNP/PDDA-modified SPCEs determined from voltammetry in this way was 1.69 (±0.34) $\times 10^{-2}$ cm^2, which corresponds to 67 (±9)% of A_{geo}. Furthermore, the AuNP surface area determined for AuNP/PDDA-modified correlates to 62 (±12)% of the electroactive surface area determined from studies with $Fe(CN)_6^{3-/4-}$, $FcMeOH/FcMeOH^+$, and $Ru(NH_3)_6^{3+/2+}$ redox couples, confirm-

ing that, though AuNPs were able to participate in electron transfer processes, their presence did not significantly improve the electroactive surface area of SPCEs.

Discussion

An increase of 102% in electroactive surface area has been reported when AuNPs are deposited on SPCEs using a PDDA-based LbL electrostatic adsorption method.[17] However, the improvement in surface area was determined from voltammetric studies that employed $Fe(CN)_6^{3-/4-}$ as the redox probe. Difficulties using $Fe(CN)_6^{3-/4-}$ as a redox couple for the characterization of some other carbon electrodes have been previously documented. For example, it has long been known that the electron transfer kinetics of $Fe(CN)_6^{3-/4-}$ are dependent on the presence and charge state of surface carboxylate groups as well as the surface history for glassy carbon and carbon paste electrodes.[41,42] Recent studies have drawn similar conclusions about the surface sensitivity of the electrochemical response of $Fe(CN)_6^{3-/4-}$ on HOPG and graphene-modified electrodes.[21–23] Here, we report evidence that suggests caution must also be practiced when characterizing SPCEs using $Fe(CN)_6^{3-}$.

Previous work with AuNP/PDDA-modified carbon electrodes[17,19] did not seem to address the possible role of PDDA in the observed peak current increase and attributed the enhancement in voltammetric signal over bare electrodes entirely to the presence of AuNPs. In studies here, voltammetric responses of PDDA-modified SPCEs were comparable to both bare and AuNP/PDDA-modified SPCEs when FcMeOH or $Ru(NH_3)_6^{3+}$ was used as the redox probe. The only significant differences between the bare and modified SPCEs were found when $Fe(CN)_6^{3-}$ was used as the redox probe, with bare SPCEs exhibiting larger ΔE_p and smaller i_p than PDDA- and AuNP/PDDA-modified SPCEs. Similarly large ΔE_p values for the $Fe(CN)_6^{3-/4-}$ redox couple have been previously reported for commercially available SPCEs[13,25,29,36] as well as HOPG[21] and graphene-modified[22,23] electrodes. The response of boron-doped diamond electrodes modified with carboxylate-functionalized graphene was found to depend on electrolyte pH with pH <8 corresponding to larger ΔE_p and smaller i_p for the $Fe(CN)_6^{3-/4-}$ redox couple.[22] Comparison of the electrochemical behavior of $Fe(CN)_6^{3-/4-}$ with SPCEs prepared from graphite and graphene inks showed larger ΔE_p for electrodes with more basal plane-like composition and lower content of oxygenated species.[29]

Interestingly, gold[43] and platinum[44] screen-printed electrodes also reportedly exhibit large ΔE_p for the $Fe(CN)_6^{3-/4-}$ redox couple. ΔE_p for the $Fe(CN)_6^{3-/4-}$ redox couple decreased from 330 to 90 mV by electrodeposition of an additional layer of gold nanoparticles onto gold screen-printed electrodes,[43] perhaps suggesting that conductive particle distribution in the cured ink and/or binder composition is also important in determining the electrochemical response of screen-printed electrodes. Indeed, ΔE_p for the $Ru(NH_3)_6^{3+/2+}$ redox couple with SPCEs prepared from custom-formulated inks was found to depend on the ratio of poly(vinyl chloride) binder to conductive pyrolytic graphite particles, with inks that featured lower percentages of binder producing smaller ΔE_p.[30] Surface treatments, such as exposure to organic solvents[26,45] and mechanical polishing,[18,31] have also been found to affect ΔE_p for common redox couples. Peak currents for $Fe(CN)_6^{3-/4-}$ increased by ~8x for SPCEs after mechanical polishing using an agate lapping hammer.[18] In a separate study, polishing SPCEs with alumina had no significant effect on electroactive surface area determined by outer-sphere redox probe $Ru(NH_3)_6^{3+/2+}$ but improved electrochemical activity toward nitrite by two-fold.[31] Treatment of SPCEs with N,N-dimethylformamide was reported to increase the electroactive surface area to 57-fold over the geometric area based on measurements with $Fe(CN)_6^{3-/4-}$.[26] However, this drastic improvement was challenged based on more modest improvements ($\leq$ 1.38-fold) found for the responses of similarly treated SPCEs toward $Ru(NH_3)_6^{3+/2+}$, capsaicin, and dihydronicotinamide adenine dinucleotide.[45]

In studies reported here, PDDA-modified SPCEs exhibited voltammetric peak currents that were comparable to those obtained with AuNP/PDDA-modified SPCEs using $Fe(CN)_6^{3-}$, FcMeOH, and $Ru(NH_3)_6^{3+}$ as redox probes. However, PDDA-modified SPCEs typically produced extra voltammetric waves for $Fe(CN)_6^{3-}$. These waves are similar to those that were reported for PDDA-modified glassy carbon electrodes and may be attributed to $Fe(CN)_6^{3-/4-}$ confined in the polymer layer at the electrode surface.[46] While CVs for AuNP/PDDA-modified SPCEs in sulfuric acid confirmed the presence of gold, the electroactive surface area that could be attributed to gold was less than the geometric surface area of the bare SPCEs and the electroactive surface areas of AuNP/PDDA-modified SPCEs that were measured using $Fe(CN)_6^{3-}$, FcMeOH, and $Ru(NH_3)_6^{3+}$ as redox probes. Overall, these results suggest that modifying the electrode surface with AuNPs by electrostatic absorption on PDDA does not result in an increase in electroactive surface area as previously reported. Rather, the surface areas of bare, PDDA-, and AuNP/PDDA-modified electrodes are all similar, and any perceived increase in surface area is likely the result of sub-optimal behavior of $Fe(CN)_6^{3-}$ as a redox probe[21–23] for the characterization of bare SPCEs.

Conclusions

LbL-modification of SPCEs provides a simple, cost-effective route to prepare nanomaterial-modified electrodes; however, care must be taken when characterizing the role and benefits of the resulting composite platforms in terms of electrochemical properties. While AuNPs immobilized on the electrode surface using an LbL strategy have been shown here to provide no improvement in the electroactive surface area over bare SPCEs, modification of SPCEs with such nanomaterials can still have advantages. Nanomaterials like AuNPs can allow ease of control of surface functionality, may be engineered to offer abundant sites for conjugation of the desired species on the electrode surface, and can exhibit catalytic properties toward some analytes and substrates. The similarities between PDDA- and AuNP/PDDA-modified SPCEs suggest that the increased $Fe(CN)_6^{3-/4-}$ peak currents observed for AuNP/PDDA-modified SPCEs compared to bare SPCEs, which have previously been attributed to the increase in surface area expected to result from the introduction of AuNPs, may be more appropriately ascribed to the effect PDDA has on making the SPCE surface more amenable for electron transfer with $Fe(CN)_6^{3-/4-}$.

Acknowledgments

Funding for this work was provided by the Office of Research and Sponsored Programs at East Tennessee State University.

References

1. J. J. Gooding, L. M. H. Lai, and I. Y. Goon, in *Chemically Modified Electrodes*, Vol. 11, eds R. C. Alkire, D. M. Kolb, J. Lipkowski, and P. N. Ross, pp. 1, Wiley-VCH Verlag GmbH & Co. KGaA, Weinheim, Germany (2009).
2. A. Manthiram, A. V. Murugan, A. Sarkar, and T. Muraliganth, *Energy Environ. Sci.*, **1**, 621 (2008).
3. G. Wang, L. Zhang, and J. Zhang, *Chem. Soc. Rev.*, **41**, 797 (2012).
4. Y. Xiang, S. Lu, and S. P. Jiang, *Chem. Soc. Rev.*, **41**, 7291 (2012).
5. G. Rydzek, Q. Ji, M. Li, P. Schaaf, J. P. Hill, F. Boulmedais, and K. Ariga, *Nano Today*, **10**, 138 (2015).
6. R. M. Iost and F. N. Crespilho, *Biosens. Bioelectron.*, **31**, 1 (2012).
7. J. F. Rusling, G. W. Bishop, N. M. Doan, and F. Papadimitrakopoulos, *J. Mater. Chem. B*, **2**, 12 (2014).
8. G. W. Bishop and J. F. Rusling, in *Nanoelectrochemistry*, eds M. V. Mirkin and S. Amemiya, pp. 469, CRC Press Taylor & Francis Group, LLC, Boca Raton, FL (2015).
9. G. Decher, *Science*, **277**, 1232 (1997).
10. J. P. Metters, R. O. Kadara, and C. E. Banks, *Analyst*, **136**, 1067 (2011).
11. M. Li, Y.-T. Li, D.-W. Li, and Y.-T. Long, *Anal. Chim. Acta*, **734**, 31 (2012).
12. R. A. S. Couto, J. L. F. C. Lima, and M. B. Quinaz, *Talanta*, **146**, 801 (2016).
13. R. O. Kadara, N. Jenkinson, and C. E. Banks, *Sens. Actuat. B*, **138**, 556 (2009).
14. S. Miserere, S. Ledru, N. Ruillé, S. Griveau, M. Boujtita, and F. Bedioui, *Electrochem. Comm.*, **8**, 238 (2006).
15. O. Bagel, B. Limoges, B. Schöllhorn, and C. Degrand, *Anal. Chem.*, **69**, 4688 (1997).
16. S. Sánchez, M. Pumera, E. Cabruja, and E. Fábregas, *Analyst*, **132**, 142 (2007).
17. B. V. Chikkaveeraiah, V. Mani, V. Patel, J. S. Gutkind, and J. F. Rusling, *Biosens. Bioelectron.*, **26**, 4477 (2011).
18. M. Yan, D. Zang, S. Ge, L. Ge, and J. Yu, *Biosens. Bioelectron.*, **38**, 355 (2012).

19. V. Mani, B. V. Chikkaveeraiah, V. Patel, J. S. Gutkind, and J. F. Rusling, *ACS Nano*, **3**, 585 (2009).
20. A. J. Bard and L. R. Faulkner, *Electrochemical Methods: Fundamentals and Applications*, 2nd Ed., John Wiley & Sons, Inc., New York (2001).
21. A. N. Patel, M. G. Collignon, M. A. O'Connell, W. O. Y. Hung, K. McKelvey, J. V. Macpherson, and P. R. Unwin, *J. Am. Chem. Soc.*, **134**, 20117 (2012).
22. M. M. Lounasvuori, M. Rosillo-Lopez, C. G. Salzmann, D. J. Caruana, and K. B. Holt, *Faraday Discuss.*, **172**, 293 (2014).
23. M. M. Lounasvuori, M. Rosillo-Lopez, C. G. Salzmann, D. J. Caruana, and K. B. Holt, *J. Electroanal. Chem.*, **753**, 28 (2015).
24. R. L. McCreery and M. T. McDermott, *Anal. Chem.*, **84**, 2602 (2012).
25. A. Morrin, A. J. Killard, and M. R. Smyth, *Anal. Lett.*, **36**, 2021 (2003).
26. A. P. Washe, P. Lozano-Sánchez, D. Bejarano-Nosas, and I. Katakis, *Electrochim. Acta*, **91**, 166 (2013).
27. C. A. Schneider, W. S. Rasband, and K. W. Eliceiri, *Nat. Methods*, **9**, 671 (2012).
28. W. Haiss, N. T. K. Thanh, J. Aveyard, and D. G. Fernig, *Anal. Chem.*, **79**, 4215 (2007).
29. E. P. Randviir, D. A. C. Brownson, J. P. Metters, R. O. Kadara, and C. E. Banks, *Phys. Chem. Chem. Phys.*, **16**, 4598 (2014).
30. N. A. Choudry, D. K. Kampouris, R. O. Kadara, and C. E. Banks, *Electrochem. Comm.*, **12**, 6 (2010).
31. L. R. Cumba, C. W. Foster, D. A. C. Brownson, J. P. Smith, J. Iniesta, B. Thakur, D. R. do Carmo, and C. E. Banks, *Analyst*, **141**, 2791 (2016).
32. R. S. Nicholson, *Anal. Chem.*, **37**, 1351 (1965).
33. H. Matsuda and Y. Ayabe, *Z. Elektrochem.*, **59**, 494 (1955).
34. P. Sun and M. V. Mirkin, *Anal. Chem.*, **78**, 6526 (2006).
35. Y. Wang, J. G. Limon-Petersen, and R. G. Compton, *J. Electroanal. Chem.*, **652**, 13 (2011).
36. P. Fanjul-Bolado, D. Hernández-Santos, P. J. Lamas-Ardisana, A. Martín-Pernía, and A. Costa-García, *Electrochim. Acta*, **53**, 3635 (2008).
37. J. Wang, M. Pedrero, H. Sakslund, O. Hammerich, and J. Pingarron, *Analyst*, **121**, 345 (1996).
38. N. Alexeyeva and K. Tammeveski, *Anal. Chim. Acta*, **618**, 140 (2008).
39. K. L. Adams, B. K. Jena, S. J. Percival, and B. Zhang, *Anal. Chem.*, **83**, 920 (2011).
40. S. Trasatti and O. A. Petrii, *Pure Appl. Chem.*, **63**, 711 (1991).
41. M. R. Deakin, K. J. Stutts, and R. M. Wightman, *J. Electroanal. Chem.*, **182**, 113 (1985).
42. K. K. Cline, M. T. McDermott, and R. L. McCreery, *J. Phys. Chem.*, **98**, 5314 (1994).
43. J. Krejci, Z. Sajdlova, V. Nedela, E. Flodrova, R. Sejnohova, H. Vranova, and R. Plicka, *J. Electrochem. Soc.*, **161**, B147 (2014).
44. A. Erlenkötter, M. Kottbus, and G.-C. Chemnitius, *J. Electroanal. Chem*, **481**, 82 (2000).
45. E. Blanco, C. W. Foster, L. R. Cumba, D. R. do Carmo, and C. E. Banks, *Analyst*, **141**, 2783 (2016).
46. M. Maizels, W. R. Heineman, and C. J. Seliskar, *Electroanalysis*, **12**, 241 (2000).